Phase Transitions in Confined Gallium Droplets

Andrea Di Cicco

UdR INFM, Dipartimento di Matematica e Fisica, Università degli Studi di Camerino, Via Madonna delle Carceri, 62032 Camerino (MC), Italy

(Received 25 March 1998)

Phase transitions in submicrometric Ga droplets confined in epoxy resin are studied by combining energy-dispersive x-ray diffraction (EDXRD), x-ray absorption fine structure, and single-energy x-ray absorption. The restricted fluid is undercooled down to 150 K while the melting point is depressed down to 254 K. Melting and freezing are sharp processes occurring with temperature broadening of 1 and 10 K, respectively. EDXRD patterns are consistent with that of β-Ga, while the stable phase at ambient conditions α-Ga is not found to exist. Appearance of γ-Ga and δ-Ga solid phases and relevance of present results to recent studies of Ga confined in porous glass are discussed. [S0031-9007(98)07341-4]

PACS numbers: 64.70.–p, 61.10.Ht

The peculiar properties of matter in confined geometries were investigated by means of experiments and calculations for a long time. In the last two decades, large efforts were devoted to the study of substances confined in various matrices with pore size in the 2–20 nm range (see, for example, [1–3] and references therein). Significant variations of specific physical properties with respect to bulk systems were found to be determined both by the restricted geometry and by the characteristics of the interaction with the porous matrix. In particular, several investigations were concentrated on the influence of restricted geometries on phase transformations in different cryogenic fluids [1–3] and low melting point metals [4,5]. Solidification and melting temperatures were found to be depressed with respect to bulk values.

Emulsions of submicrometric gallium droplets buried in solidified epoxy resin, used in recent x-ray absorption fine structure (XAFS) studies [6–8], provide a nice example of a restricted liquid system. Droplets are confined in unconnected regions of approximate spherical shape with sizes in the 100–1000 nm range, and therefore interface interaction and finite-size effects can be neglected due to the relatively large dimensions of the confined particles. The undercooling capabilities of micrometric metal droplets, with typical undercooling temperatures ΔT_- in the range 0.13–0.33 times the absolute melting temperature T_m, are well known [9]. In particular, large undercooling rates $\Delta T_-/T_m \sim 0.325$ [10] are easily obtained for Ga droplets and evidence for exceptional undercooling $\Delta T_-/T_m \sim 0.5$ was also reported [11]. In our previous XAFS experiment we observed extremely large undercooling effects in confined Ga droplets [7], but due to the insufficient energy resolution and to the intrinsic short-range nature of the technique we were not able to detect any phase transition.

In this Letter, I report the results of an accurate investigation about phase transitions in confined submicrometric Ga droplets by combining energy-dispersive x-ray diffraction (EDXRD), high resolution XAFS, and single-energy x-ray absorption [12] as a function of temperature. The present study is aimed to shed light on the peculiar freezing and melting properties of gallium under restricted geometry [5–8] using such unconventional techniques.

Gallium droplets were emulsified into epoxy resin at about 320 K. The solidified emulsion was shaped in the form of slabs of appropriate thickness for x-ray absorption and diffraction measurements (see Refs. [6,7]). Characterization of samples was performed by using optical and scanning electron (SEM) microscopes. Distribution of droplet size for the present sample (hereafter referred to as sample F) was found to follow quite closely a log-normal model [7] with mean value of $\bar{\lambda} \sim -0.95$ and variance $\sigma_\lambda^2 \sim 0.27$ for the logarithm $\lambda \equiv \ln \delta$ of the diameters δ (measured in μm) of the droplets. Present statistics was carried out by using 1296 particles detected by SEM imaging. EDXRD patterns as a function of temperature were recorded at beam line DW11A (Laboratoire pour l'Utilisation du Rayonnement Electromagnetique, Orsay) using the white synchrotron radiation beam emitted by the DCI wiggler. Accurate XAFS experiments were performed at the European Synchrotron Radiation Facility (ESRF) on the bending magnet beam line BM29 using a high-stability fixed-exit double-crystal Si(311) monochromator achieving a resolution of about 0.5 eV FWHM at the Ga K-edge with a 0.3 mm vertical slit. Temperature was ramped continuously using a closed-cycle He cryostat with typical rates of -0.05 and $+0.1$ K/s for cooling and warming scans, respectively.

In Fig. 1 the EDXRD normalized patterns for sample F are reported as a function of temperature (downstroke). The weak background due to the epoxy was measured separately and subtracted from the energy patterns. Bragg peaks start to appear below 150 K, as verified by a series of EDXRD scans. Above this temperature, Ga droplets can remain in the liquid state on the typical time scales of the experiment (tenths of minutes at least).

In Fig. 2, upper panel, four EDXRD patterns at 80, 200, 250, and 260 K recorded during a single upstroke of a thermal cycle are shown. The Bragg peaks are found to

 0031-9007/98/81(14)/2942(4)$15.00

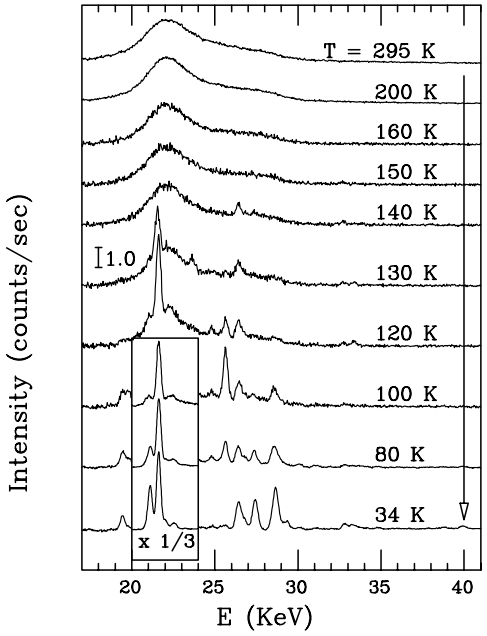

FIG. 1. EDXRD normalized patterns for the emulsion of Ga droplets (sample F) recorded for decreasing temperatures. Integration times were about 1800 s for the 295, 200, 80, and 34 K patterns and about 300 s for the others. Intense Bragg peaks at low temperatures are reduced by a factor of 3 in the inset.

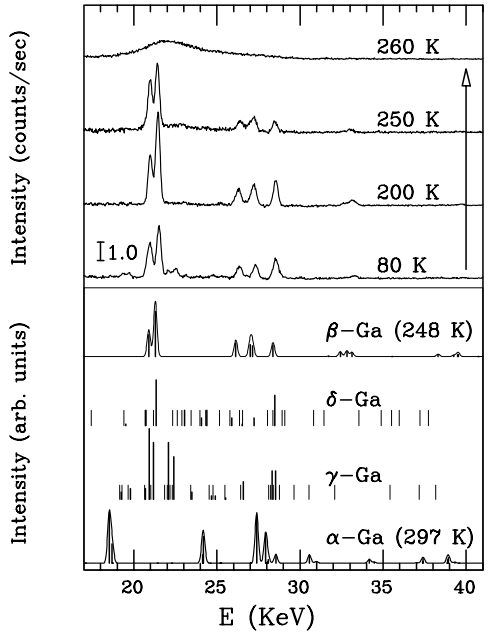

FIG. 2. Upper panel: EDXRD normalized patterns of sample F at 80, 200, 250, and 260 K recorded increasing the temperature. Lower panel: Calculated EDXRD spectra for the stable α [13] and metastable β [14] phases (solid lines). Position [15] and relative estimated intensity [16] of γ-Ga and δ-Ga Bragg peaks are also reported.

disappear invariably at $T_m = 255 \pm 5$ K, well below the melting temperature of Ga at ambient conditions ($T_m = 302.9$ K). The calculated EDXRD spectra for the stable α [13] and metastable β [14] phases in normal conditions are shown in Fig. 2, lower panel. Calculations were carried out taking into account the energy dependence of the atomic scattering factor and a realistic energy pattern of the source and absorbance from the sample.

Looking at the calculations, it is clear that the presence of the α phase is ruled out by present x-ray diffraction experiments, confirming previous XAFS data [6]. On the other hand, the most important peaks observed in experimental data are in agreement with the β-Ga pattern. The shift observed at lower temperatures is due to the shortening of the average unit cell parameters. In particular, both the 34 K pattern in Fig. 1 and the 80 K pattern in Fig. 2 show all of the peaks of the β-Ga calculation in the whole energy range. Weaker features around 19.5, 22, 22.5, 25, 25.5 and 29 KeV are consistent with interplanar distances of the γ-Ga and δ-Ga metastable phases [15]. In Fig. 2, lower panel, γ-Ga and δ-Ga diffraction lines previously observed in Ga dispersions are reported for comparison along with their estimated intensity (see Ref. [16]) and position [15]. No clear evidence for other previously observed metastable phases [16] is found in the present experiment. The small peaks assigned to γ-Ga and δ-Ga are quite evident in the process of freezing (Fig. 1) but are less pronounced at 34 K and disappear by heating the sample again in a range of temperature between 200 and 250 K (Fig. 2, upper panel).

In Fig. 3, upper panels, the Ga K-edge x-ray absorption fine structures $\alpha(E)$ are shown for a thermal cycle of sample F including a downstroke from 308 to 27 K and a successive upstroke from 28 to 275 K. XAFS spectra appear to change smoothly revealing no drastic changes of the average local structure as a function of temperature, in agreement with previous results [6–8]. However, present performances and stability of the monochromatic beam allow one to study tiny variations of the absorption spectra. In Fig. 3, lower panels, some significative difference spectra $\Delta\alpha(E) = \alpha_{T_2} - \alpha_{T_1}$ are reported (T_2 and T_1 temperatures are indicated in the figure). Looking at the difference spectra for decreasing temperatures (left), a clear change in the absorption is obtained between 165 and 126 K, monitored by the deep minimum in the $\alpha_{152\mathrm{K}}$-$\alpha_{126\mathrm{K}}$ difference spectrum at about 10.379 KeV. This corresponds to the undercooled liquid-solid phase transition. Above this temperature, in the liquid phase, there is an almost continuous variation of the fine structure associated with changes in the local ordering. The observed differences in the XAFS spectra of liquid and undercooled Ga show the large short-range sensitivity of the technique. Below 150 K difference spectra do not show significative variations, apart from modest edge shift and thermal vibration effects (lowest spectrum in the lower-left panel of Fig. 3). In the lower-right panel of Fig. 3 some interesting $\Delta\alpha$ spectra obtained increasing the temperature are shown. Modest changes as a function of temperature are observed in the 100–240 K

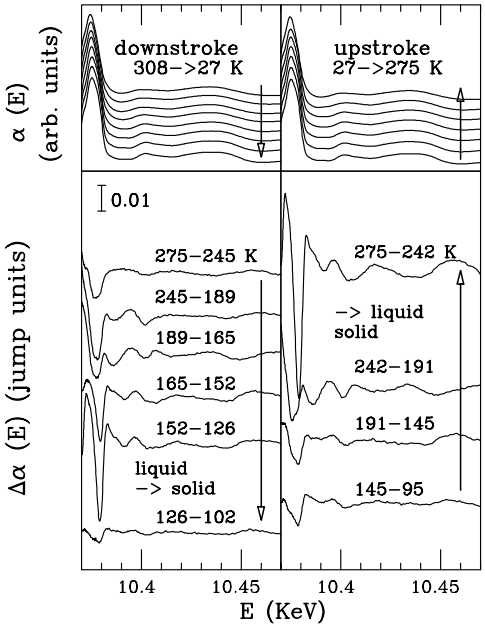

FIG. 3. Upper panels: X-ray absorption coefficient $\alpha(E)$ of sample F obtained decreasing ($T = 308$, 275, 245, 189, 152, 102, 53, and 27 K, left) and increasing (27, 54, 95, 145, 190, 241, 275 K, right) the temperature. Lower panels: Difference signals $\Delta\alpha(E)$ of XAFS spectra recorded along the downstroke (left) and the upstroke (right) of a thermal cycle.

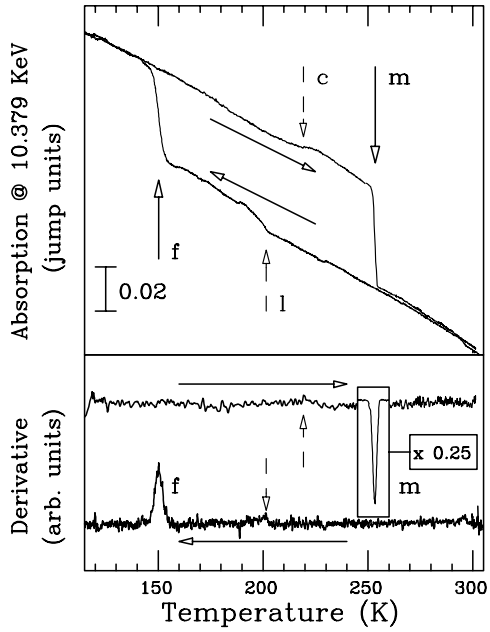

FIG. 4. Upper panel: Temperature scan of the absorption coefficient at constant energy showing a clear hysteresis loop. Melting and freezing are indicated by arrows labeled as m and f, respectively. Lower panel: Derivative of the temperature scan shown in the upper panel.

range (and below) as shown by the last three curves in the bottom part of the panel, which are associated with solid gallium. The $\alpha_{242\mathrm{K}}$-$\alpha_{191\mathrm{K}}$ spectrum, however, shows a remarkable fine structure, which could be associated to a solid-solid phase transition. The large change observed above 242 K is certainly associated with the solid-liquid phase transition for Ga droplets.

A deep insight into those phase transitions can be obtained by recording the absorption coefficient at constant energy, specifically selected in order to evidence structural changes [12]. In Fig. 4, upper panel, a temperature scan of the absorption coefficient at constant energy $E = 10.379$ KeV of sample F is reported. This energy gives the maximum contrast between solid and liquid phase XAFS as shown in Fig. 3, upper panel. A clear hysteresis loop is evidenced during the thermal cycle (arrows in Fig. 4). A first broad transition is evidenced below 200 K (l) along the downstroke, while a rather sharp freezing process (f) takes place around 150 K. The temperature scan is smooth and shows no hysteresis below 120 K down to about 30 K. Along the upstroke, a first smooth transition occurs at about 220 K (c). The second sharp transition occurs at about 255 K and is associated with melting (m) of confined solid Ga. The derivative curves shown in Fig. 4, lower panel, allow us to evidence such transitions: solidification f occurs at a mean temperature $T_f = 150$ K with about 10 K FWHM, while the melting temperature results to be $T_m = 254$ K with a width of about 1 K.

The present solidification temperature corresponds to extreme undercooling rates $\Delta T_-/T_m \sim 0.5$ with respect to the α-Ga melting temperature and $\Delta T_-/T_m \sim 0.4$ with respect to the actual T_m of sample F. The same undercooling temperature is observed also on different Ga emulsions in epoxy resin and appears to be a characteristic limiting temperature for undercooling of confined Ga droplets. This result is in nice agreement with the metastability limit $T_L = 150 \pm 1$ K in liquid gallium, which defines the minimum crystallization temperature [11]. This limit was determined by inelastic neutron diffraction measurements [11] on Ga droplets prepared using the Turnbull's emulsion technique [9,10]. Recent molecular dynamics simulations of rapidly quenched Ga essentially confirmed this result [17].

Melting of sample F is shifted about 50 K with respect to the normal α-Ga melting point at ambient pressure. As a matter of fact, confined Ga droplets crystallize according to different phases which are metastable at ambient conditions. The main reason is that Ga is an ice-type element for which the density of the stable α-Ga solid phase near melting (5.904 g/cm^3) is much lower than that of the liquid phase ($\sim$6.095 g/cm^3 near the melting point). On the contrary, estimated densities near melting of the metastable phases β-Ga ($\sim$6.23 g/cm^3), δ-Ga ($\sim$6.22 g/cm^3), and γ-Ga ($\sim$6.20 g/cm^3) are larger and compatible with available room for isolated droplets in the liquid phase. Therefore, geometrical confinement prevents solidification in the stable phase at ambient conditions and favors extreme undercooling.

The melting point of confined Ga droplets $T_m \sim 254$ K is in qualitative agreement with that of β-Ga at atmospheric pressure $T_m = 256.8$ K. On the other hand, it is in excellent agreement with that of δ-Ga ($T_m = 253.7$ K [14]). However, the sharpness of the XAFS change associated with melting (see Fig. 4) and the peculiar EDXRD pattern (Fig. 2) better supports a solid-liquid transition from a single phase, which is likely to be β-Ga.

Interpretation of the other features observed in the single-energy x-ray temperature scan shown in Fig. 4 is less obvious. The first smooth feature at about 200 K (arrow *l* in Fig. 4) upon lowering the temperature can be due either to a change in the structural or electronic properties of the undercooled liquid or to crystal nucleation occurring in a minority of Ga droplets. This last assignment is not supported by EDXRD scans (Fig. 1) although tiny Bragg peaks could be hidden in the liquid background. The more fascinating interpretation of a liquid-liquid transition [18,19] involving tiny changes of either the average structure or the electron density of states requires further investigations. The second smooth feature (arrow *c* in Fig. 4) observed at about 220 K could be assigned to a solid-solid phase transition. This transition could be associated with a transformation from γ or δ phases to the β phase. This interpretation is supported by the lack of Bragg peaks typical of those phases (see Fig. 2) above $T \sim 200$ K. Moreover, the relatively low melting points of γ-Ga and δ-Ga, $T_m = 237.5$ K and $T_m = 253.7$ K, respectively, are consistent with a tendency to reach more stable phases around these temperatures.

Comparison of present results with previous experiments on confined Ga in porous glass [5] is also quite interesting. Gallium was found to be superconducting below about 7 K, which is compatible with the presence of β-Ga and γ-Ga in such a confined system [15]. The anomalies in the conductivity and specific heat at about 220 and 250 K measured on warming [5] are likely to have the same origin of those observed using x-ray absorption and diffraction in the present work.

Present results show that Ga droplets confined in epoxy resin experience sharp phase transitions both during cooling and warming processes. The undercooled liquid-solid transition is located at 150 K while melting takes place at about 254 K. Direct evidence for those transitions is obtained by using EDXRD, XAFS, and single-energy x-ray absorption temperature scans which gave consistent and unambiguous results. Differences between bulk Ga and this restricted system appear to be largely controlled by geometrical confinement. In fact, the density of the stable α-Ga solid phase is lower than that of liquid Ga and freezing is observed to occur in denser solid phases, metastable in normal conditions. The sample preparation technique can be easily extended to other low-melting metals or substances. Experimental techniques are found to be particularly sensitive for discovering and studying phase transitions and can be used on a variety of solid and liquid systems. Further experimental investigations on restricted fluids using these methods are stimulated by this work.

J. P. Itiè and A. Filipponi are kindly acknowledged for skillful operation of experimental facilities and assistance at LURE and ESRF. I also thank M. Minicucci, G. Aquilanti, and M. Taglienti for their help during beam time and G. Cantalupo for SEM characterization (Camerino). ESRF hospitality as a visiting scientist and INFM funding are gratefully acknowledged.

[1] J. Warnock, D. D. Awschalom, and M. W. Schafer, Phys. Rev. Lett. **57**, 1753 (1986).
[2] P. E. Sokol *et al.*, Appl. Phys. Lett. **61**, 777 (1992).
[3] E. Molz, A. P. Y. Wong, M. W. Chan, and J. R. Beamish, Phys. Rev. B **48**, 5741 (1993).
[4] Yu. A. Kumzerov, A. A. Nabereznov, S. B. Vakhrushev, and B. N. Savenko, Phys. Rev. B **52**, 4772 (1995).
[5] C. Tien *et al.*, Phys. Rev. B **54**, 11 880 (1996); C. Tien *et al.*, Solid State Commun. **104**, 753 (1997).
[6] A. Di Cicco and A. Filipponi, J. Non-Cryst. Solids **156–158**, 102 (1993).
[7] L. Ottaviano, A. Filipponi, and A. Di Cicco, Phys. Rev. B **49**, 11 749 (1994).
[8] A. Di Cicco and A. Filipponi, Europhys. Lett. **27**, 407 (1994).
[9] D. Turnbull, J. Appl. Phys. **21**, 1022 (1950); J. Chem. Phys. **20**, 411 (1952).
[10] Y. Miyazawa and G. M. Pound, J. Cryst. Growth **23**, 45 (1974).
[11] L. Bosio and C. G. Windsor, Phys. Rev. Lett. **35**, 1652 (1975).
[12] A. Filipponi *et al.*, J. Phys. Condens. Matter **10**, 235 (1998).
[13] C. S. Barrett and F. J. Spooner, Nature (London) **207**, 1382 (1965).
[14] L. Bosio and A. Defrain, Acta Crystallogr. Sect. B **25**, 995 (1969).
[15] L. Bosio, A. Defrain, and M. Dupont, J. Chim. Phys. **68**, 542 (1971).
[16] R. D. Heyding, W. Keeney, and S. L. Segel, J. Phys. Chem. Solids **34**, 133 (1973).
[17] S.-F. Tsay, Phys. Rev. B **50**, 103 (1994).
[18] C. A. Angell, S. Borick, and M. Grabow, J. Non-Cryst. Solids **205–207**, 463 (1996).
[19] V. V. Brazhkin, R. N. Voloshin, S. V. Popova, and A. G. Umnov, J. Phys. Condens. Matter **4**, 1419 (1992).